COUPLING CLIMATE CONDITIONS, SEDIMENT SOURCES AND SEDIMENT TRANSPORT IN AN ALPINE BASIN

Riccardo Rainato[a*], Lorenzo Picco[a, b], Marco Cavalli[c], Luca Mao[d], Andrew J. Neverman[e], Paolo Tarolli[a]

[a] *Department of Land, Environment, Agriculture and Forestry, University of Padova, Padova, Italy;*

[b] *RiNA Research Center for Natural and Anthropogenic Risks, Institute of Civil Works, Universidad Austral de Chile, Valdivia, Chile;*

[c] *CNR-IRPI, Corso Stati Uniti 4, 35127 Padova, Italy;*

[d] *Department of Ecosystems and Environment, Pontificia Universidad Catòlica de Chile, Santiago, Chile;*

[e] *Physical Geography Group, Institute of Agriculture & Environment, Massey University, Palmerston North, New Zealand.*

[*]Corresponding author: Tel.: + 39 0498272695; fax: +39 0498272686; e-mail address: riccardo.rainato@unipd.it

ABSTRACT

In a fluvial system, mountain basins control sediment export to the lowland rivers. Hence, analysis of erosion processes and sediment delivery patterns in mountain basins is a key factor for many applications such as land-use management, hazard assessment, and infrastructure design. Several studies have investigated the alterations triggered by recent climatic change on the hydrological regime, whilst only a few works have explored the consequences on fluvial sediment dynamics. Here we combined and analyzed the quasi-unique dataset of climatic conditions, landform response, and sediment export produced, since 1986 in the Rio Cordon basin (5 km^2, Eastern Italian Alps) to examine the sediment delivery processes occurring in the last three decades. The temperature, precipitation, and fluvial sediment fluxes in the basin were analyzed using continuous measurement executed by a permanent monitoring station, while the evolution of sediment source areas was investigated using three sediment source inventories. The results showed that during the period 1986-1993 the sediment fluxes (339 Mg yr^{-1}) reflected the stable trend of the climatic conditions. The period between the first and second source inventory (i.e. 1994-2006) was characterized by climatic fluctuations and by the occurrence of high magnitude floods. Nevertheless, a limited increase in the extent of sediment source areas was detected, suggesting that the increased sediment export (759 Mg yr^{-1}) was mainly driven by in-channel sediment supply. Notwithstanding the marked climate warming and the increased precipitation, a weak source area evolution and a reduction in sediment export (237 Mg yr^{-1}) were observed

during the period 2007-2015. In particular, the higher rainfall did not result in an intensification of flood events, stressing the absence of hillslope-channel connectivity.

Key-words: Alpine basin; climate change; sediment sources evolution; source area; sediment connectivity; sediment transport.

INTRODUCTION

The land degradation acting in high mountain basins can lead to significant alterations to the local fluvial system, influencing channel morphology, sediment dynamics, natural hazards, and biodiversity; changes that can be rapidly transmitted downstream (Keesstra *et al.*, 2005; Liebault *et al.*, 2005, Comiti *et al.*, 2011; Moretto *et al.*, 2014; Picco *et al.*, 2016; Tarolli & Sofia, 2016). Erosion processes in mountain basins are influenced by several factors such as climate, topography, lithology and paraglacial adjustments (Montgomery & Buffington, 1997; Jones, 2000; Le Pera & Sorriso-Valvo, 2000; Carrivick & Chase, 2011; Fischer *et al*., 2014). The key role played by climatic conditions was particularly evident in recent decades due to climate change (Bennett *et al.*, 2013). Climate change may strongly affect not only water discharge (Menzel & Burger, 2003), riverine habitat and water quality (Ashmore & Church, 2001), but also soil erosion and subsequent sediment fluxes along different channel networks (Michael *et al.*, 2005; Syvitski *et al.*, 2005). For instance, Zhu *et al.* (2008) reported changes in sediment fluxes in the Longchuanjiang catchment (China) after changes in temperature and rainfall. Moreover, increasing attention has been devoted to the direct relationship between changing climate and rising flood risk (Milly *et al.*, 2002; Hirabayashi *et al.*, 2013). In alpine basins sediment production and export seem to be affected by recent climatic variations. These effects could be particularly marked since, during the last century, the alpine range experienced a temperature increase (~ 2°C) higher than central Europe (Hinderer *et al.*, 2013). Climate variability, especially in terms of temperature and precipitation, can lead to temporal trends in the hydrological regime and sediment dynamics, with significant implications for channel morphology and landform dynamics (Morche *et al*., 2012; Geilhausen *et al*., 2013; Baewert & Morche, 2014; Micheletti & Lane, 2016). Rainfall and temperature regimes cause erosion and weathering in the basin, controlling sediment production (Buendia *et al.,* 2016). In conjunction with soil infiltration capacity (Harden & Scruggs, 2003), temperature variations control the erosion and dispersion of sediments from potential sources, especially by periodical

freeze-thaw processes (López-Tarazón *et al.*; 2012). Sass & Oberlechner (2012), analyzing the Austrian rockfall inventory (252 events over the last century), observed higher rockfall activity during colder years. The author attributed this tendency to bedrock contraction and cleft propagation occurring with low temperatures. In glaciated basins, climate warming may lead increased water yield (Micheletti & Lane, 2016), as well as increased sediment export by inducing permafrost degradation (Bennett *et al.*, 2013) or by favoring the development of an enhanced sediment connectivity, as observed in the Haut Glacier d'Arolla (Swiss Alps) by Lane *et al.* (2017). On the other hand, precipitation patterns act both on sediment erosion along the hillslope (Rossi *et al.*, 2010) and on the runoff regime (Bocchiola, 2014). Several studies have explored the effects of recent climatic shifts on the hydrological regime (Geilhausen *et al.*, 2013; Bennett *et al.*, 2014), whilst the impacts on fluvial sediment dynamics have been poorly investigated due to a limited number of long-lasting monitoring programs (Lane *et al.*, 2017). Very few mountain basins are instrumented to investigate contemporary climate and hydrological trends, along with changes in sediment source areas and sediment fluxes, and thus, few quantitative long-term datasets (> 10 yr) are available. Studies which do capture these datasets were mainly conducted in glaciated or formerly glaciated basins, rarely focusing on non-glacial catchments. Analyzing two small and partially glaciated mountain catchments located in the Canton of Valais (Swiss Alps), Micheletti & Lane (2016) observed that climate variations occurring in the last three decades led to an increase in water yield and sediment transport capacity, but this trend was not accompanied by an increase in sediment export due to low hillslope-channel connectivity. Nonlinear behavior between rainfall, discharge, and sediment export was observed by Lana-Renault *et al.* (2007) in a small unglaciated Pyrenees basin, highlighting the complexity of sediment dynamics in the catchment. The authors observed that rainfall is not the most significant controlling factor of sediment yield, stressing the importance of the continuity of cascading sediment flux, and thus, of sediment connectivity (e.g., Cavalli *et al.*, 2013; Heckmann & Schwanghart, 2013). This evidence seems to suggest that in dynamic systems such as mountain catchments climatic conditions permit only partial description of sediment export. By producing change in sediment storage landforms, erosion processes can lead to the creation of sediment sources, that in the mountain basins can vary from large debris flow-channels and -deposits to shallow landslides (Lenzi *et al.*, 2003; Messenzehl *et al.* 2014; Cavalli *et al.*, 2017). Thus, by acting on the source areas, sediment erosion strongly controls fluvial sediment transport, which is essentially related to hydrological and sediment supply

conditions (Mao *et al.*, 2009; Recking, 2012). In particular, the source areas control the amount of material delivered to the channel network, also defining in-channel features and influencing sediment mobility conditions (Yu *et al.*, 2009, Piton & Recking, in press). This is particularly evident in small mountain basins, where the type and extent of sediment sources may strongly influence the nature, magnitude, and efficiency of fluvial transport processes (Schuerch *et al.*, 2009; Rainato *et al.*, 2017). The material supplied by the slopes may reach the channel network or not, depending on coupling\decoupling relationships between sediment sources and the channel network. In light of this, the sediment yield exhibited by the mountain basins, further to the climatic and hydrological conditions, is strongly controlled by the connectivity between source areas and the channel network (Bracken *et al.*, 2015; Dell'Agnese *et al.*, 2015). The presence/absence of hillslope-channel network coupling, and its degree, can influence the temporal response of the catchment to sediment supply variation. Indeed, a lagged response of basins, despite increased hillslope erosion, can be due to the absence of sediment connectivity between the slopes and drainage network (Bennett *et al.*, 2013; Messenzehl *et al.,* 2014). In this respect, small mountain basins offer a great opportunity to assess the sediment cascade continuity, since here hillslope-channel network coupling is characterized by rapid connectivity, both temporally and spatially (Sanjuán *et al.*, 2016).

This work aims to investigate the climate trends, evolution of sediment source areas, and fluvial sediment fluxes in an alpine basin over the last three decades. The quasi-unique monitoring program maintained in the Rio Cordon basin since 1986 allows us to: i) analyze the shifts in temperature and precipitation regimes, and ii) evaluate the response of sediment source areas; specifically, in terms of source evolution. After defining the sediment connectivity acting in the catchment, changes observed in the climate trends and source areas were compared to the sediment fluxes independently recorded at the outlet of the basin. Hence, the quasi-unique dataset provided by the Rio Cordon monitoring program was used to shed further light on the central, but only rarely analyzed, cause-effect coupling between climate forcing and sediment delivery patterns, providing insights to be compared with other monitored catchments.

MATERIAL AND METHODS

Study area

Rio Cordon is a mountain basin located in the eastern Italian Alps (Dolomites). The catchment (Figure 1) covers an area of 5 km^2 and the elevation ranges from 1,763 to 2,763 m.a.s.l.. While the average slope is 27°, this is locally exceeded along the subvertical cliffs located in the upper part of the basin, where slopes higher than 45° were detected (Trevisani *et al.*, 2010). The basin is part of the Southern Calcareous Alps with prevalent dolomite and volcanic conglomerates (Wengen group) in the upper part, whereas sandstones and calcareous–marly rocks (Buchenstein group) characterize the lower part. Additionally, a wide presence of quaternary deposits (i.e. moraines, scree, and landslide accumulations) can be observed throughout the study area (Cavalli *et al.*, 2016). In the basin three main soil-types are noticeable: brown earth-soil is widely spread, while the skeleton- and organic-soils are mainly present on the partially vegetated steep slopes and in the lower vegetated areas, respectively (Lenzi *et al.*, 2004).

####### Figure 1 #######

In terms of climate, the Rio Cordon basin is characterized by alpine climatic conditions with an average annual precipitation of 1,150 mm. Between November and April, the precipitation occurs mainly as snowfall, while during the rest of the year rainfall prevails. Consequently, the runoff exhibits a typical nivo-pluvial regime with snowmelt during the May-June period and periodical floods in summer and autumn due to rainstorm and persistent rainfall, respectively.

In relation to the sediment cascade, the basin exhibits a wide presence of sediment sources, which consist mainly of debris flow-channels and -deposits, landslides, and talus slopes. Overall, these areas cover roughly 13% of the basin (Ferrato *et al.*, 2017). Due to the presence of a low-gradient belt located at approximately 2,200 m.a.s.l., the upstream sources provide a minor contribution to the sediment export (Dalla Fontana & Marchi, 2003). Currently, the basin appears to be characterized by a low-moderate sediment supply condition (Rainato *et al.*, 2017). The Rio Cordon stream has developed its torrential system mainly over quaternary moraine and scree deposits. The average slope of the main channel is 17%, featuring a rough streambed with step-pool morphology and large boulders. The grain size distribution of surface material exhibits the percentiles $D_{16}/D_{50}/D_{84}$ equal to 29/114/358 mm, respectively. Currently, the streambed is strongly armoured with the subsurface D_{50} (38 mm) three-fold lower in respect to the surface D_{50} (Mao *et al.*, 2010). The bankfull discharge was estimated by Lenzi *et al.* (2006) as equal to 2.30 $m^3 s^{-1}$.

In terms of land use, alpine grasslands and shrubs cover 60% and 15% of the basin area, respectively. Non-vegetated areas and bare rocks (i.e. subvertical cliffs) are present in 14% of the catchment, while the forested areas (*Picea abies* and *Larix decidua*) cover only the lower part, accounting for 6%. Anthropogenic influences are limited to a small number of hikers and seasonal grazing of bovine, donkeys, and sheep. Also, a total absence of artificial structures can be observed along the river network.

Climate data

In the Rio Cordon basin, two meteorological stations were set up by the Veneto Region (Experimental Centre of Arabba) and currently managed by ARPA Veneto. In 1986, at 1,763 m.a.sl., the Rio Cordon station was established. Here, rainfall is continuously gathered by a heated rain gauge, while air temperature, atmospheric pressure, relative humidity, and solar radiation have been constantly recorded since 1994. An additional meteorological station (Mondeval di Sopra station) equipped with a rain gauge and an air temperature sensor was established in 1992 at 2,130 m.a.sl. Climatic conditions are recorded hourly at both stations. This continuous monitoring provides a detailed description of the rainfall regime for the last three decades in the basin. For the aim of this paper the time series produced by the heated rain gauge installed in the Rio Cordon station was used because it covers the entire period analyzed (i.e. 1986-2015). In relation to the air temperature regime, the two meteorological stations located in the basin do not provide data over the entire 1986-2015 period. In fact, the Mondeval di Sopra and Rio Cordon stations started to measure air temperature in 1992 and 1994, respectively. To address this issue, the temperature time series produced for Caprile was investigated. The Caprile meteorological station (ARPA Veneto) is located only 6 km south-west of the Rio Cordon basin, at 1,008 m.a.s.l. (Figure 1a). The Caprile time series was used since it is the closest meteorological station with continuous climate monitoring during the period 1986-2015.

Sediment sources data

During the 1986-2015 period, three inventories of potential sediment sources were created in the Rio Cordon basin. These investigations were carried out by a collaboration between University of Padova and CNR-IRPI that aimed to characterize the sources in terms of spatial extent, type, and location. The first inventory is dated summer 1994 and is based both on geomorphic field surveys, performed using measuring tape and

altimeter, and on interpretation of aerial photographs (1: 25,000 scale). The resulting inventory map (1:10,000 scale) was later integrated in to a GIS environment to permit comparison with subsequent inventories (Cavalli *et al.*, 2016).

The second inventory was carried out in late summer 2006 (Cavalli *et al.*, 2016). First, the sediment sources characterization was performed through geomorphic field mapping with a hand-held GPS receiver, laser rangefinder, measuring tape, and digital photo camera. Additionally, in October 2006 a LiDAR flight was carried out to produce a Digital Terrain Model (DTM). The high resolution (1 m) enabled investigation and mapping of sources not detected in the field due to their non-accessible location.

The most recent inventory was produced in 2016. Similar to the previous inventories, the 2016 mapping was started by field surveys performed with a GPS. To identify sediment sources located in unreachable areas photo interpretation was conducted on images derived by Bing® satellite service and WMS service for AGEA (i.e. Italian Agricultural Payments Agency). In both cases the images used are from 2012, but the absence of significant variations in the unreachable areas has permitted use of the images in the 2016 inventory.

Over the three inventories, the source areas were geometrically surveyed (without any evaluation of thickness) and classified into seven types (Figure 2):

- debris flow-channel: all channels affected by debris flow (Figure 2a). Even triggering areas, if not clearly attributable to other processes (e.g. shallow landslides), were classified in this source type. Due to the access limitations of steep channels in which debris flow processes occur, the geometry of this sediment source type was approximately mapped in the field;
- debris flow-deposit: depositional areas related to debris flow events (Figure 2a). A mud-flow deposit (Figure 2b) derived from a landslide of fine-medium grain size material (Figure 2f) occurred during the snowmelt-induced flood of May 11, 2001, but for simplicity was included in the debris flow-deposit category;
- erosional area: is a sediment source type widespread on catchment slopes (Figure 2c). This type refers to areas affected by erosional processes: all unvegetated areas or with poor grass cover, with marked evidence of erosion activity not related to landslides were classified as erosional area. In the Rio Cordon basin, rill erosion is the most common form of surficial erosion and originates by both steep gradient

slopes and anthropic causes, particularly the intensive cattle grazing that leads to the progressive grass cover degradation;

- eroded stream bank: channel network banks presenting erosion, mainly triggered by the water flow (Figure 2d). The distinction between eroded stream bank and erosional area is justified by the great importance for sediment dynamics played by sources belonging to the former type and due to their direct link with the channel network;
- landslide: steep debris-mantled slope where the action of gravity is the primary driving force. All the detected landslides initiated in sediment (Figure 2f);
- rockfall deposit: depositional areas related to rockfall events;
- active talus: sediment eroded from rock cliffs temporarily stored as scree deposits on talus slopes (Figure 2g).

Moreover, small wetlands areas (Figure 2h) which display an important role in the deposition and entrapment of sediments were also surveyed but not considered as sediment sources.

Further details on the Rio Cordon inventories and on the methodology used can be found in Cavalli *et al.* (2016) and Ferrato *et al.* (2017).

####### Figure 2 #######

Sediment connectivity

In order to depict spatial patterns of sediment connectivity in the catchment, a topography-based index of sediment connectivity (IC) (Cavalli *et al.*, 2013) was applied. In this work the index, expressing the potential connection between hillslope and selected targets, is aimed at evaluating the potential linkage between the hillslope domain and basin outlet. IC was computed through SedInConnect 2.0 (Crema *et al.*, 2015) using a LiDAR-derived DTM at 1 m resolution (Cavalli *et al.*, 2016) and a weighting factor based on surface roughness. Further details on the methodology can be found in Cavalli *et al.* (2013).

Fluvial sediment fluxes data

In the Rio Cordon basin, the fluvial sediment fluxes have been continuously recorded since 1986 by a long-term monitoring program. The program was established through a collaboration between University of

Padova and Veneto Region which in 1985 led to the construction of a permanent monitoring station designed for the continuous measurement of water discharge (Q), suspended sediment load (SSL) and bedload (BL). Located at 1,763 m.a.s.l. (i.e. basin outlet), the monitoring station measures Q by two water gauges and a sharp-crested weir, while SSL is assessed by two turbidimeters. Specifically, the sampling time resolution is 1-hour during ordinary flow conditions ($Q < 1$ m^3 s^{-1}), and increases to 5 minutes for $Q > 1$ m^3 s^{-1}. In the period 1986-2015, a time fraction of 15% presented data gaps in relation to the water discharge or suspended load. An inclined metallic grid enables the coarse material ($D > 20$ mm) of bedload events to be separated from the water flow. Once separated, the bedload falls into a storage area where 24 ultrasonic sensors measure the transport rate. To achieve a higher estimation accuracy, since 2012 a Terrestrial Laser Scanner has been used to estimate the amount of coarse material deposited in the storage area. The volume data obtained is then converted to mass using a sediment density of 2.65 Mg m^3 and a material porosity of 35%.

In relation to the cause-effect coupling between climate forcing and sediment delivery patterns, the research activities performed in the Rio Cordon alpine basin led to the availability of a quasi-unique dataset. Overall, the dataset (1986-2015) permits the investigation of sediment source response (i.e. sediment source data) to long-term climate trends (i.e. climate data). In turn, it is possible to analyze whether, and how, the trends of climatic condition and evolution of sediment source areas cause a response in fluvial sediment fluxes (i.e. fluvial sediment fluxes data).

RESULTS

Climate trends

The trends of the monthly average air temperature recorded by the Caprile (1,008 m.a.s.l.), Rio Cordon (1,763 m.a.s.l.) and Mondeval di Sopra (2,130 m.a.s.l.) meteorological stations during 2011-2015 (Figure 3a) show the presence of an elevation gradient. The temperature shifts that occurred in the Rio Cordon basin appear to be well described by the Caprile station. Comparing the hourly temperatures recorded in the 2011-2015 period a roughly linear relationship can be observed between the temperature recorded by the Caprile station and the Rio Cordon and Mondeval di Sopra measurements (Figure 3b). According to the Pearson correlation coefficients (r), Rio Cordon and Caprile temperatures were strongly correlated ($r = 0.96$, $p < 0.01$). A significant correlation ($r = 0.92$, $p < 0.01$) also exists between Mondeval di Sopra and Caprile.

Therefore, due to the absence of a long-term temperature time series record in the Rio Cordon basin, the Caprile dataset was used in this study as it covers the study period.

####### Figure 3 #######

The mean annual air temperature for Caprile over the 1986-2015 period is 6.9 °C (Table 1). The trend of mean annual temperature as deviation from the 1986-2015 average (i.e. annual temperature anomaly) seems to suggest the occurrence of three distinct stages during the study period. Initially, between 1986 and 1991, the temperature constantly exhibits a negative anomaly, with annual averages lower than the 30-year average (Figure 4). In the period 1986-1991, the mean temperature (6.5 °C) was clearly lower than the 1986-2015 average, with the coldest year recorded in 1991 with an anomaly of -0.7 °C (i.e. mean annual = 6.2 °C).

####### Figure 4 #######

Since 1992, the temperature regime was characterized by a high inter-annual variability with a succession of positive and negative anomalies that lasted until 2006. In this period, the warmest year was recorded in 1994 with a temperature anomaly of +0.4 °C. On the other hand, the highest negative anomaly equal to -0.8 °C (i.e. mean annual = 6.1 °C) was measured both in 1995 and 2005. Such years were the coldest of the last 30 years. Since 2007, the mean annual temperatures were constantly above the 1986-2015 average, with an increase in positive anomalies (Figure 4). The only exception to this trend was 2010, with a negative anomaly of -0.4 °C. From 2007 the mean temperature was 7.3 °C, corresponding to an increase of 5.8% in respect to the 1986-2015 average. Also, in 2015 the highest temperature of the whole 1986-2015 period was recorded, with a positive anomaly equal to +1.1 °C.

####### Table 1 #######

Rainfall recorded by the Rio Cordon meteorological station shows that between 1986 and 1999 the annual precipitation was relatively constant, with limited inter-annual variability (Figure 5). Since 2000, significant shifts in the precipitation regime were observed. In 2000, 2001 and 2002 annual precipitation was recorded as 1,409 mm, 949 mm and 1,358 mm, respectively (Table 1). These amounts clearly differ from each other and from the 1986-2015 average (i.e. 1,157 mm/year). From 2003 to 2006 a period characterized by an almost constant significant reduction in rainfall was observed. During this 4-year period the average precipitation was 942 mm, and 2004 (841 mm) was the driest year of the last three decades. Since 2007 a long period of increased precipitation was recorded. Particularly, the mean annual precipitation between

2007 and 2015 was 1392 mm, 20% higher than the 1986-2015 average. The wettest year of the entire study period was 2014 (1,757 mm) (Table 1). The increase observed since 2007 was partially offset by 2015, when the annual rainfall was 1,015 mm.

####### Figure 5 #######

Trend of hillslope sediment sources

In 1994, 292 sources were detected, covering a total area of 498,265 m^2, with an average extent of 1,706 m^2. In terms of extent, active talus slopes (174,423 m^2) was the predominant source type. In 1994, the 24 mapped talus areas exhibited an average surface area of 7,268 m^2 and were detected mainly at the foot of the subvertical cliffs located in the upper part of the basin (Figure 6). Erosional areas were also particularly vast (160,241 m^2), with an average extent (2,428 m^2) notably lower than the active talus. More than 160 landslides were identified in the basin by the 1994-inventory, extending over a total area of 149,197 m^2 (Table 2). Compared with these source types, the areas affected by stream bank erosion and debris flow (channels and deposits) were approximately two orders of magnitude lower, covering 5,517 m^2 and 8,887 m^2, respectively. Overall, in 1994 the active source areas covered 9.9% of the basin surface. Additionally, 13 wetlands, extending on average 3,588 m^2, were detected (Table 2).

####### Table 2 #######

On the other hand, in 2006, more than 400 source areas were identified, covering 648,554 m^2. The average area (1,548 m^2) slightly decreased from 1994. As in the first inventory, the largest source type in 2006 was active talus, which are mainly located in the upper part of the basin (Figure 6). The 26 active talus exhibited an average area (8,084 m^2) larger than in the previous inventory. More than 190 landslides were mapped in 2006, with several new sources activated along the left side of the lower basin (i.e. South-Southeast). In this inventory, the landslides showed an average surface area comparable to that observed in 1994. In total, this source type accounted for a surface area of 191,797 m^2. Erosional area covers a similar areal extent, but this type was characterized by larger individual sources (average area = 1,745 m^2). However, compared to the results obtained in 1994, erosional area is less extensive (- 39%). Since the 2006-inventory, debris flow-channels and -deposits were separately mapped (Table 2). This classification highlighted that, with respect to debris flow-channels, debris flow-deposits were larger both in terms of total and average area. Overall, 78

source areas were related to debris flow processes, covering an area (71,623 m^2) clearly higher than in 1994. Such an increase is not evident in the average area, which remains similar to that observed in the previous inventory. Also in 2006, eroded stream bank was observed in the lower extent of the basin (3,902 m^2), with 22 sediment sources covering on average just 177 m^2. Overall, in 2006 the active source areas covered 12.9% of catchment area. Total and average area of wetlands was fully comparable to that observed in 1994 (Table 2).

Finally, the source area inventory performed in 2016 showed an extent comparable to 2006. Despite a slight decrease in the average area (- 4%), the active talus remained the main source type. In 2016, a considerable portion of the basin remains affected by landslides, which slightly increased in total area (+ 2%) while decreased in average surface area (- 5%). An opposite trend can be observed in the erosional area. Compared to 2006, debris flow-channels and debris flow-deposits showed a different evolution. In fact, the debris flow-channels increased both in terms of total (+ 23%) and average area (+ 17%), while debris-flow deposits decreased in both. Notably, eroded stream bank reduced in extent, with the average area nearly two fold lower compared to 2006. Interestingly, in 2016 a massive rockfall deposit (20,676 m^2) was detected along the northeastern cliffs (Figure 6). The deposit obliterated more than 10,000 m^2 of previously classified active talus (Table 2). Overall, during this last period the extent of the catchment covered by sediment source areas remains exactly the same. Similarly, the wetlands exhibited only a slight reduction in terms of average area (-8%).

In general, it should be noted that the 1994 sediment source database is characterized by a lower accuracy and completeness with respect to the most recent ones. Accordingly, the comparative quantitative analysis with the 2006 and 2016 databases needs to be carried out in a critical manner, as reported in Cavalli *et al.* (2016).

####### Figure 6 #######

Sediment connectivity analysis

The map of IC highlighting the potential degree of linkage between hillslope and catchment outlet is presented in Figure 7. This analysis highlights that high connectivity values characterize the lower sector of the catchment, which is characterized by steep slopes and a narrow valley. In this part of the basin, most of

the sediment sources on hillslopes can be considered well connected to the outlet. Different spatial patterns of connectivity can be observed in the middle and upper parts of the study area. Lower IC values suggest that the low-gradient belt and several depressions characterizing the middle part of the basin strongly affect the sediment fluxes, favoring deposition and retainment of sediment and, thus, decoupling sediment sources located in these areas from the outlet.

####### Figure 7 #######

Fluvial sediment fluxes trends

The long lasting monitoring of fluvial sediment transport in the Rio Cordon enables us to assess the sediment fluxes which occurred during the last 30 years. During the period 1986-2015, a total of 15,110 Mg was exported from the basin to the monitoring station as suspended sediment load and bedload (Figure 8). The total load recorded corresponds to an annual sediment yield equal to 504 Mg yr^{-1} (i.e. 100 t km^{-2} yr^{-1}).

####### Figure 8 #######

Overall, during the study period the suspended load fraction (SSL_f = 0.79) clearly prevails over the bedload fraction (BL_f = 0.21). In terms of temporal trends, the sediment yield reflects the high inter-annual variability exhibited by suspended load and bedload. Between 1986 and 1993, the annual sediment yield was continuously lower than 1,000 Mg yr^{-1}, except in 1991, with SSL_f always above 0.60. As a consequence of the September 1994 exceptional event, more than 4,000 t were exported from the basin in 1994. In this year, bedload (1,543 t) and suspended load (2,524 t) exhibited the highest magnitude ever recorded. Between 1994 and 2003, significant fluctuations can be observed in the sediment fluxes (Figure 8), with the annual sediment yield varying by two orders of magnitude. Specifically, the annual sediment export at the monitoring station ranged between 12 t recorded in 2003 to 1,743 t assessed in 2001. Large annual shifts can be observed also in the partitioning, with SSL_f varying from 0.59 to 1.00 recorded in 1998 and 1997, respectively. Since 2003, the annual sediment yields were consistently lower than 600 Mg yr^{-1}. In the last 13 years an evident decrease of bedload yield was observed with magnitude constantly < 100 Mg yr^{-1} and BL_f < 0.30. A minor interruption to this trend was recorded in 2014 (BL_f = 0.31), when 118 t of coarse material were exported from the basin.

DISCUSSION

Despite the high complexity of the mountain system and the complex interplay of different controlling factors (i.e. topography, runoff, sediment availability), the availability of the quasi-unique dataset provided by the Rio Cordon monitoring program permits us to assess the cause-effect coupling between climate forcing and sediment delivery patterns. Specifically, the continuous measurement of climatic conditions and sediment fluxes were analyzed in combination with the three sediment source inventories representative of sediment availability in the basin in the last 30 years. The analysis focused on the trends exhibited during the inter-periods, i.e. 1986-1993, 1994-2006 and 2007-2015. In the Rio Cordon, the climate and fluvial sediment flux datasets are generally of good quality since they are produced by monitoring stations constantly managed by ARPA Veneto (Rainato *et al.*, 2017). Between 1986 and 1993, the climatic conditions appear relatively stable both in terms of temperature and rainfall. During this period the mean temperature was 6.6 °C, with the standard deviation (*SD* = 0.30 °C) of the annual values confirming that no significant fluctuations occurred. Likewise, rainfall exhibited a low inter-annual variability (*SD* = 136 mm), with an average precipitation equal to 1,063 mm. Similar to what was observed in the small and formerly glaciated Val Müschauns (Swiss Alps) by Messenzehl *et al.* (2014), the sediment source area inventories in the Rio Cordon are generally dominated by active talus, erosional area and landslides. In 1994, the sources appeared altogether quite distant from the channel network (Figure 6). Fluvial sediment fluxes showed a stable trend during the 1986-1993 period, similar to the trend exhibited by the climatic conditions. The mean annual sediment yield was 339 Mg yr^{-1}, with clear prevalence of *SSL* fraction (SSL_f= 0.85). Climatically, the 1994-2006 period was somewhat similar to the 1986-1993 period, but exhibited larger inter-annual fluctuations. Indeed, the average temperature (6.7 °C) was in line with that observed in the previous phase, while *SD* increased to 0.44 °C. The same trend can be observed in precipitation, with mean and *SD* equal to 1,053 mm and 190 mm, respectively. In addition to the climatic conditions, during the period 1994-2006 source area change was strongly affected by the occurrence of high magnitude/low frequency flood events. Particularly, the September 1994 exceptional event strongly impacted the Rio Cordon basin, creating new source areas and reactivating old ones (Rainato *et al.*, 2017), while in May 2001 a large mudflow occurred along a small tributary located in the lower part of the basin, creating an extended debris fan (~ 4,176 m^3) (Lenzi *et al.*, 2004). The 2006 source inventory showed a noticeable increase (+ 30%) in terms of total area. This change

is affected by a certain degree of uncertainty, due to the use of geomorphic field mapping to characterize the sediment sources and, particularly, by the different methodology used in the 2006 inventory survey compared to the 1994 survey (Cavalli *et al.*, 2016). As argued by several authors (Bishop *et al.*, 2012; Messenzehl *et al.*, 2014), field mapping is subject to a certain error range, rarely computed, and mainly due to the subjectivity and the uncertainty derived by time-consuming field operations. Nevertheless, geomorphic field mapping is largely used to investigate sediment cascades in mountain environments, enabling researchers to obtain qualitative results scarcely achieved by quantitative approaches (Messenzehl *et al.*, 2014). The effect of using a diverse methodology between 1994 and 2006 is clearly evident in the number of sources detected and in the total area (Table 2). Principally, the increase observed is due to the higher accuracy used to describe the debris flow type (+ 62,736 m^2). Nevertheless, a certain increase in this type seems to have occurred, as suggested by the increased average surface. Interestingly, the climatic fluctuations and the high magnitude/low frequency floods increased the number, extent, and average area of landslides. Such variation is particularly evident in the lower part of the basin along the slopes next to the channel network (Figure 6). Compared to that noted in 1994, in 2006 a higher number of erosional areas was observed along the hillslopes, but they were smaller on average (Figure 6). This evolution could be explained by climate forcing between 1994-2006, or by extensive cattle grazing occurring in the catchment (Cavalli *et al.*, 2016). Notwithstanding the high magnitude/low frequency floods, eroded stream bank was reduced compared to 1994. This decrease seems to suggest that the channel network rapidly exhausted the sediment availability here created by the high magnitude events. In 12 years (1994-2006), eroded stream bank was stabilized or reduced by supplying and increasing the transport efficiency of the post-September 1994 floods (Rainato *et al.*, 2017). In the 1994-2006 period, the partitioning (BL_f = 0.15) was fully comparable to that observed in the 1986-1993 period. In this sense, the increase of active talus and landslides did not lead to a variation in the *BL* and *SSL* fractions. The partitioning clearly varied only in the years with high magnitude/low frequency floods such as 1994 (BL_f = 0.38), 1998 (BL_f = 0.41), and 1999 (BL_f = 0.31), i.e. under conditions of effective connectivity between source areas and channel network. On the other hand, sediment export exhibited a strong increase, with a mean annual sediment yield equal to 759 Mg yr^{-1}. In this sense, the key role played by the exceptional September 1994 flood is evident. However, sediment export remains high (i.e. 484 Mg yr^{-1}) even excluding 1994 from the analysis. The shifts observed in the climatic

conditions and the relative change of sediment source areas seems to only partially explain the augmented sediment export measured in the 1994-2006 period, stressing the role played by the in-channel sediment availability resulting from the removal of the armour layer and bedforms by the September 1994 flood.

The 2007-2015 period showed an evident increase both in terms of average temperature (7.3 °C) and mean precipitation (1,392 mm). This increasing trend appears to be more stable in the temperature data, exhibiting an inter-annual variability (*SD* = 0.48 °C) in line with that observed in the 1994-2006 period. On the other hand, precipitation was characterized by significant annual fluctuations (*SD* = 256 mm). This climate forcing resulted in a very limited sediment source change. The number of landslides increased slightly, while the decreased extent of active talus was mainly due to the effect of the 2016 rockfall, which obliterated ~ 10,000 m^2 previously classified as active talus (Table 2). In addition to the climatic conditions, cattle grazing concentrated in specific areas of the basin could explain the variation in erosional area, which decreased in total count (-15%) but increased in average area. In the period 2007-2015, the increased precipitation was not accompanied by an intensification of flood occurrence, which may explain the reduction observed in eroded stream bank compared to the 1994-2006 period. The decrease of fluvial bedload fraction (BL_f = 0.07) seems to somehow reflect this sediment source evolution. Generally, the climatic trend recorded in the 2007-2015 period did not produce an increase in erosion processes in the Rio Cordon basin. This hypothesis also seems to be supported by the increase in stabilized areas and by the reduction of small wetlands (Table 2). The absence of a significant change of sediment source areas due to climate forcing, combined with the armoring of the channel network, seems to explain the significant decrease observed in sediment export during the 2007-2015 period, when the mean annual sediment yield was 237 Mg yr^{-1}. Compared to glaciated basins, non-glacial catchments usually exhibit lower erosion rates but higher sediment exports due to confined valley morphology and, hence, by the high transport efficiency of the stream (Hinderer, 2001; Mao *et al.*, 2009). Notwithstanding the unglaciated nature of the Rio Cordon basin, the sediment fluxes were generally limited, stressing the key role played by the evident sediment disconnectivity (Figure 7). Particularly, the upper part of the basin is clearly decoupled from the outlet, reducing the potential contribution of active talus, i.e. the dominant source type. Overall, a large number of current sediment sources are located away from the channel network, in areas not usually coupled to the main channel (Figure 6). A comparable degree of sediment disconnectivity is normally observed in glaciated alpine basins due to the presence of hanging

valleys or inherited glacial landforms (Cavalli *et al*., 2013; Heckmann & Schwanghart, 2013; Messenzehl *et al.*, 2014; Micheletti & Lane, 2016). In the Rio Cordon basin, the low-gradient belt located at 2,200 m.a.s.l acts as the main buffer within the sediment cascade continuity. Consequently, the current state of disconnectivity appears quite stable in time, since it is imposed by steady geomorphic conditions. As demonstrated by several authors (Messenzehl *et al.*, 2014, Micheletti *et al.*, 2015) the presence of a buffer within the sediment cascade makes it difficult to fully comprehend the consequence of recent climate change on sediment fluxes. In this sense, the effect of decoupling between sediment sources and the channel network was clearly observed in the period 2007-2015, when the increase in temperature and precipitation was not reflected by an intensification of sediment export. Clear evidence of this scenario was also the rockfall which occurred in 2016, affecting a large surface and mobilizing massive amounts of material, but not resulting in any effects in terms of fluvial sediment fluxes. Moreover, a high transport efficiency was achieved only recently in 2012 and 2014 when floods supported by an effective hillslope-channel network coupling occurred (Rainato *et al.*, in press). In light of ongoing climate change, it will be interesting to assess how long this disconnected status will last. The potential change induced by the climate on erosion processes (Stott & Mount, 2007) could lead to an enhanced sediment cascade condition and, in turn, to a lagged and massive response of the basin (Messenzehl *et al.*, 2014).

FINAL REMARKS

This study investigated the climate trends, the relative sediment source areas evolution, and the fluvial sediment export response exhibited by an alpine basin over the last three decades. The research activities performed in the Rio Cordon basin led to the availability of a quasi-unique dataset based on the continuous measurement of temperature, precipitation, fluvial sediment fluxes, and three sediment source inventories established in 1994, 2006, and 2016. The analysis focused on the trends exhibited during the periods 1986-1993, 1994-2006, and 2007-2015. In terms of climatic conditions, three distinct climate forcing stages can be observed in the periods analyzed: a relatively stable phase (1986-1993), a period characterized by temperature and rainfall fluctuations (1994-2006), and a more recent warmer and wetter phase (2007-2015). In the 1986-1993 period, the fluvial sediment fluxes reflected the stable trend exhibited by the climatic conditions. In the subsequent 1994-2006 period, the average temperature and precipitation were in line with

that previously observed, although with higher inter-annual variability. Notwithstanding the climate forcing and the occurrence of high magnitude/low frequency floods that strongly influenced the source areas, between 1994 and 2006 the Rio Cordon basin showed relatively limited erosion activity. Hence, the climatic conditions and the change in sediment source areas can only partially explain the significant increase in sediment export recorded in the 1994-2006 period. In this sense, the sediment availability resulting from armour layer and bedform removal appears crucial to describing the sediment fluxes during this period, stressing the key role of in-channel sediment supply. In the recent period 2007-2015 a marked climate warming accompanied by increased precipitation was observed. This climate forcing did not affect the evolution of sediment landforms, with sediment source extent remaining similar between 2006 and 2016. The absence of a significant response from sediment source areas and the restoration of the channel armour layer can describe the limited sediment fluxes observed during the last decade. In particular, the increased temperature and precipitation were not accompanied by an increase in flood occurrence and magnitude, stressing the evident sediment disconnectivity. In the Rio Cordon, as in similar mountain basins, it will be interesting to monitor and investigate how long the current (dis)connectivity status will be maintained, particularly in light of climate change, that could rapidly alter the sediment dynamics observed so far.

In this work, the results suggest a nonlinear behavior between climatic condition, landform response and sediment dynamics, emphasizing the high complexity of the mountain systems. Very few unglaciated mountain basins are instrumented to investigate contemporary climate trends, the change of sediment source areas, and sediment export. As a result, quantitative long-term data are particularly rare. The quasi-unique monitoring program maintained in the Rio Cordon basin since 1986 enabled us to analyze whether, and how, the trends of climatic condition and sediment landform evolution can influence fluvial sediment fluxes, stressing the role played by the presence/absence of hillslope-channel connectivity and shedding further light on the complex sediment delivery processes acting in mountain basins.

ACKNOWLEDGEMENTS

This research was funded by the University of Padova Research Projects ‘Sediment transfer processes in an Alpine basin: sediment cascades from hillslopes to the channel network-BIRD167919’, and "Source areas

and channel networks. Increasing the knowledge on sediment connectivity around alpine basins" DOR1701834/17. We would like to thank Prof. Mario Aristide Lenzi since the article has benefited from discussion with him, as well as Matteo Cesca (ARPA Veneto) for the technical support. Many thanks go to Alison Garside for revising the English. We are grateful to Karoline Messenzehl and David Morche for their constructive comments, which helped us to improve the manuscript.

REFERENCES

Ashmore PE, Church M. 2001. The impact of climate change on rivers and river processes in Canada. *Bulletin of the Geological Survey of Canada* **555**: 1-48.

Baewert H, Morche D. 2014. Coarse sediment dynamics in a proglacial fluvial system (Fagge River, Tyrol). *Geomorphology* **218**: 88-97.

Bennett G, Molnar P, McArdell B, Schlunegger F, Burlando P. 2013. Patterns and controls of sediment production, transfer and yield in the Illgraben. *Geomorphology* **188**: 68–82.

Bennett G, Molnar P, McArdell B, Burlando P. 2014. A probabilistic sediment cascade model of sediment production, transfer and yield in the Illgraben. *Water Resources Research* **50**: 1225-1244. DOI: 10.1002/2013WR013806.

Bishop MP, James LA, Shroder Jr JF, Walsh SJ. 2012. Geospatial technologies and digital geomorphological mapping: Concepts, issues and research. *Geomorphology* **137**: 5-26.

Bocchiola D. 2014. Long term (1921-2011) changes of Alpine catchments regime in Northern Italy. *Advances in Water Resources* **70**: 51-64.

Bracken LJ, Turnbull L, Wainwright J, Bogaart P. 2015. Sediment connectivity: a framework for nderstanding sediment transfer at multiple scales. *Earth Surface Processes and Landforms* **40**: 177-188. DOI: 10.1002/esp.3635, 2015.

Buendia C, Vericat D, Batalla RJ, Gibbins CN. 2016. Temporal dynamics of sediment transport and transient in-channel storage in a highly erodible catchment. *Land Degradation & Development* **27**: 1045-1063. DOI: 10.1002/ldr.2348.

Carrivick JL, Chase SE. 2011. Spatial and temporal variability in the net mass balance of glaciers in the southern Alps, New zealand. *New Zealand Journal of Geography and Geophysics* **54**: 415-429.

Cavalli M, Trevisani S, Comiti F, Marchi L. 2013. Geomorphometric assessment of spatial sediment connectivity in small Alpine catchments. *Geomorphology* **188**, 31–41.

Cavalli M, Tarolli P, Dalla Fontana G, Marchi L. 2016. Multi-temporal analysis of sediment source areas and sediment connectivity in the Rio Cordon catchment (Dolomites). *Rendiconti Online Società Geologica Italiana* **39**, 27-30.

Cavalli M, Goldin B, Comiti F, Brardinoni F, Marchi L. 2017. Assessment of erosion and deposition in steep mountain basins by differencing sequential digital terrain models. *Geomorphology* **291**, 4-16. DOI: 10.1016/j.geomorph.2016.04.009

Comiti F, Da Canal M, Surian N, Mao L, Picco L, Lenzi MA. 2011. Channel adjustments and vegetation cover dynamics in a large gravel bed river over the last 200 years. *Geomorphology* **125**: 147–159.

Crema S, Schenato L, Goldin B, Marchi L, Cavalli M. 2015. Toward the development of a stand-alone application for the assessment of sediment connectivity. *Rendiconti Online della Società Geologica Italiana* **34**, 58-61.

Dalla Fontana G, Marchi L. 2003. Slope-area relationships and sediment dynamics in two alpine streams. *Hydrological Processes* **17**(1): 73-87.

Dell'Agnese A, Brardinoni F, Toro M, Mao L, Engel M, Comiti F. 2015. Bedload transport in a formerly glaciated mountain catchment constrained by particle tracking, *Earth Surface Dynamics* **3**: 527–542. DOI: 10.5194/esurf-3-527-2015, 2015.

Ferrato C, De Marco J, Tarolli P, Cavalli M. 2017. An updated source areas inventory in the Rio Cordon catchment (Dolomites). *Rendiconti Online Società Geologica Italiana*.

Fischer M, Huss M, Hoelzle M. 2014. Surface elevation and mass changes of all Swiss glaciers 1980-2010. *Cryosphere Discussions* **8**: 4581-4617.

Geilhausen M, Morche D, Otto JC, Schrott L. 2013. Sediment discharge from the proglacial zone of a retreating Alpine glacier. *Zeitschrift für Geomorphologie* **57**: 29-53.

Harden CP, Scruggs PD. 2003. Infiltration on mountain slopes: A comparison of three environments. *Geomorphology* **55**: 5-24.

Heckmann T, Schwanghart W. 2013. Geomorphic coupling and sediment connectivity in an alpine catchment - Exploring sediment cascades using graph theory. *Geomorphology* **182**: 89–103. DOI: 10.1016/j.geomorph.2012.10.033.

Hinderer M. 2001. Late Quaternary denudation of the Alps, valley and lake fillings and modern river loads. *Geodinamica Acta* **14**, 231-263.

Hinderer M, Kastowski M, Kamelger A, Bartolini C, Schlunegger C. 2013. River loads and modern denudation of the Alps — a review. *Earth-Science Reviews* **118**: 11–44.

Hirabayashi Y, Mahendran R, Koirala S, Konoshima L, Yamazaki D, Watanabe S, Kim H, Nakae S. 2013. Global flood risk under climate change. *Nature Climate Change* **3**: 816-821.

Jones AP. 2000. Late Quaternary sediment sources, storage and transfers within mountain basins using clast lithological analysis: Pineta Basin, central Pyrenees, Spain. *Geomorphology* **34**: 145-161.

Keesstra SD, van Huissteden J, Vandenberghe J, Dam OV, de Gier J, Pleizier ID. 2005. Evolution of the morphology of the river Dragonja (SW Slovenia) due to land-use changes. *Geomorphology* **69**: 191–207.

Lana-Ranault N, Regüés-Muñoz D, Martí-Bono CE, Beguería S, Latrón J, Nadal-Romero E, Serrano-Muela P, García-Ruiz JM. 2007. Temporal variability in the relationships between precipitation, discharge and suspended sediment concentration in a small Mediterranean mountain catchment. *Nordic Hydrology* **38**: 139–150.

Lane SN, Bakker M, Gabbud C, Micheletti N, Saugy JN. 2017. Sediment export, transient landscape response and catchment-scale connectivity following rapid climate warming and Alpine glacier recession. *Geomorphology* **277**, 210-227. DOI: 10.1016/j.geomorph.2016.02.015.

Le Pera E, Sorriso-Valvo M. 2000. Weathering, erosion and sediment composition in a high-gradient river, Calabria, Italy. *Earth Surface Processes and Landforms* **25**: 277-292.

Lenzi MA, Mao L, Comiti F. 2003. Interannual variation of suspended sediment load and sediment yield in an alpine catchment. *Hydrological Science Journal* **48**(6): 899–915.

Lenzi MA, Mao L, Comiti F. 2004. Magnitude-frequency analysis of bed load data in an Alpine boulder bed stream. *Water Resourced Research* **40**(7): 1–12.

Leopold LB. 1994. A view of the river. Harvard University Press: Cambridge (USA). 298 pp.

Liébault F, Gomez B, Page M, Marden M, Peacock D, Richard D, Trotter CM. 2005. Land-use change, sediment production and channel response in upland regions. *River Research and Applications* **21**: 739-756.

López-Tarazón JA, Batalla RJ, Vericat D, Francke T. 2012. The sediment budget of a highly dynamic mesoscale catchment: the River Isábena. *Geomorphology* **138**: 15-28.

Mao L, Cavalli M, Comiti F, Marchi L, Lenzi MA, Arattano M. 2009. Sediment transfer processes in two Alpine catchments of contrasting morphological settings. *Journal of Hydrology* **364**(1–2): 88–98.

Mao L, Comiti F, Lenzi MA. 2010. Bedload dynamics in steep mountain rivers: insights from the Rio Cordon Experimental Station (Italian Alps). In: Gray, J.R., Laronne, J.B., Marr, J.D.G. (Eds.), Bedload-surrogate Monitoring Technologies, U.S. Geological Survey Scientific Investigations Report 2010–5091: pp. 253–265.

Menzel L, Burger G. 2002. Climate change scenarios and runoff response in the Mulde catchment (Southern Elbe, Germany). *Journal of Hydrology* **267** (1–2): 53-64.

Messenzehl K, Hoffmann T, Dikau R. 2014. Sediment connectivity in the high-alpine valley of Val Müschauns, Swiss National Park - linking geomorphic field mapping with geomorphometric modelling, *Geomorphology* **221**: 215–229.

Michael A, Schmidt J, Enke W, Deutschlander T, Malitz G. 2005. Impact of expected increase in precipitation intensities on soil loss results of comparative model simulations. *Catena* **61** (2–3): 155-164.

Micheletti N, Lane SN, Lambiel C. 2015. Investigating decadal scale geomorphic dynamics in an Alpine mountain setting. *Journal of Geophysical Research: Earth Surface* **120**: 2155-2175.

Micheletti N, Lane SN. 2016. Water yield and sediment export in small, partially glaciated Alpine watersheds in a warming climate. *Water Resources Research* **52**(6): 4924-4943. DOI: 10.1002/2016WR018774.

Milly PCD, Wetherald RT, Dunne KA, Delworth TL. 2002. Increasing risk of great floods in a changing climate. *Nature* **415**: 514-517.

Montgomery DR, Buffington JM. 1997. Channel-reach morphology in mountain drainage basins. *Geol. Soc. Am. Bull.* **109**: 596 – 611.

Morche D, Haas F, Baewert H, Heckmann T, Schmidt KH, Becht M. 2012. Sediment transport in the proglacial Fagge River (Kaunertal/Austria). In: Collins, A.L., Golosov, V., Horowitz, A.J., Lu, X., Stone, M., Walling, D.E., Zhang, X. (Eds.), Erosion and Sediment Yields in the Changing Environment. IAHS Press Wallingford, *IAHS Publication* **356**: 72–81.

Moretto J, Rigon E, Mao L, Picco L, Delai F, Lenzi AM. 2014. Channel adjustments and island dynamics in the Brenta River (Italy) over the last 30 years. *River Research and Applications* **30**: 719-732.

Nijssen B, O'Donnell G, Hamlet A, Lettenmaier D. 2001. Hydrologic sensitivity of global rivers to climate change. *Climatic Change* **50** (1–2): 143-175.

Picco L, Sitzia T, Mao L, Comiti F, Lenzi MA. 2016. Linking riparian woody communities and fluviomorphological characteristics in a regulated gravel-bed river (Piave river, Northern Italy). *Ecohydrology* **9**: 101-12.

Piton G, Recking A. in press. The concept of travelling bedload and its consequences for bedload computation in mountain streams. *Earth Surface Processes and Landforms*. DOI: 10.1002/esp.4105.

Rainato R, Mao L, Garcia-Rama A, Picco L, Cesca M, Vianello A, Preciso E, Scussel GR, Lenzi MA. 2017. Three decades of monitoring in the Rio Cordon instrumented basin: sediment budget and temporal trend of sediment yield. *Geomorphology* **291**, 45-56. DOI: 10.1016/j.geomorph.2016.03.012.

Rainato R., Mao L., Picco L., in press. Near-bankfull floods in an Alpine stream: effects on the sediment mobility and bedload magnitude. *International Journal of Sediment Research.* DOI: 10.1016/j.ijsrc.2017.03.006.

Recking A. 2012. Influence of sediment supply on mountain streams bedload transport. *Geomorphology* **175-176**: 139–150. DOI: 10.1016/j.geomorph.2012.07.005.

Rossi M, Witt A, Guzzetti F, Malamud BD, Peruccacci S. 2010. Analysis of historical landslides in the Emilia–Romagna region, northern Italy. *Earth Surface Processes and Landforms* **35**: 1123-1137.

Sanjuán Y, Gómez-Villar A, Nadal-Romero E, Álvarez-Martínez J, Arnáez J, Serrano-Muela MP. Rubiales J M, González-Sampériz P, García-Ruiz JM. 2016. Linking land cover changes in the sub-alpine and montane belts to changes in a torrential river. *Land Degradation and Development* **27**: 179–189. DOI: 10.1002/ldr.2294.

Sass O, Oberlechner M. 2012. Is climate change causing increased rockfall frequency in Austria? *Natural Hazards and Earth System Science* **12**: 3209-3216

Schuerch P, Densmore AL, McArdell BW, Molnar P. 2006. The influence of landsliding on sediment supply and channel change in a steep mountain catchment. *Geomorphology* **78:** 222–235.

Stott T, Mount N. 2007. Alpine proglacial suspended sediment dynamics in warm and cool ablation seasons: Implications for global warming. Journal of Hydrology **332**, 259–270.

Syvitski JPM, Kettner AJ, Peckham SD, Kao SJ. 2005. Predicting the flux of sediment to the coastal zone: application to the Lanyang watershed, Northern Taiwan. *Journal of Coastal Research* **21** (3): 580-587.

Tarolli P, Sofia G. 2016. Human topographic signatures and derived geomorphic processes across landscapes. *Geomorphology* **255**: 140–161.

Trevisani S, Cavalli M, Marchi L. 2010. Reading the bed morphology of a mountain stream: a geomorphometric study on high-resolution topographic data. *Hydrology and Earth System Sciences* **14**: 393–405. DOI: 10.5194/hess-14-393-2010.

Yu G, Wang Z, Zhang K, Chang T, Liu H. 2009. Effect of incoming sediment on the transport rate of bed load in mountain streams. *International Journal of Sediment Research* **24**: 260–273.

Zhu YM, Lu XX, Zhou Y. 2008. Sediment flux sensitivity to climate change: a case study in the Longchuanjiang catchment of the upper Yangtze River, China. *Global and Planetary Change* **60**: 429-442.

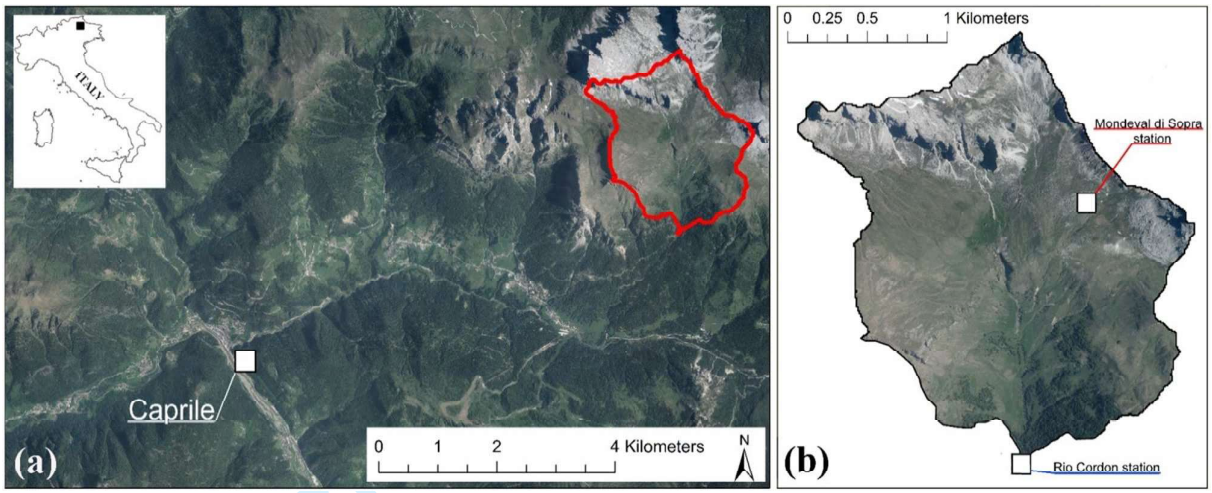

Figure 1: Location of the Rio Cordon basin (red outline) with respect to Caprile (a), and the Mondeval di Sopra and Rio Cordon stations in the basin (b). "Rio Cordon station" identifies both the meteorological and sediment transport monitoring station. The latitude-longitude (WGS84) of the Rio Cordon monitoring station are: 46.4505 N and 12.0953 E.

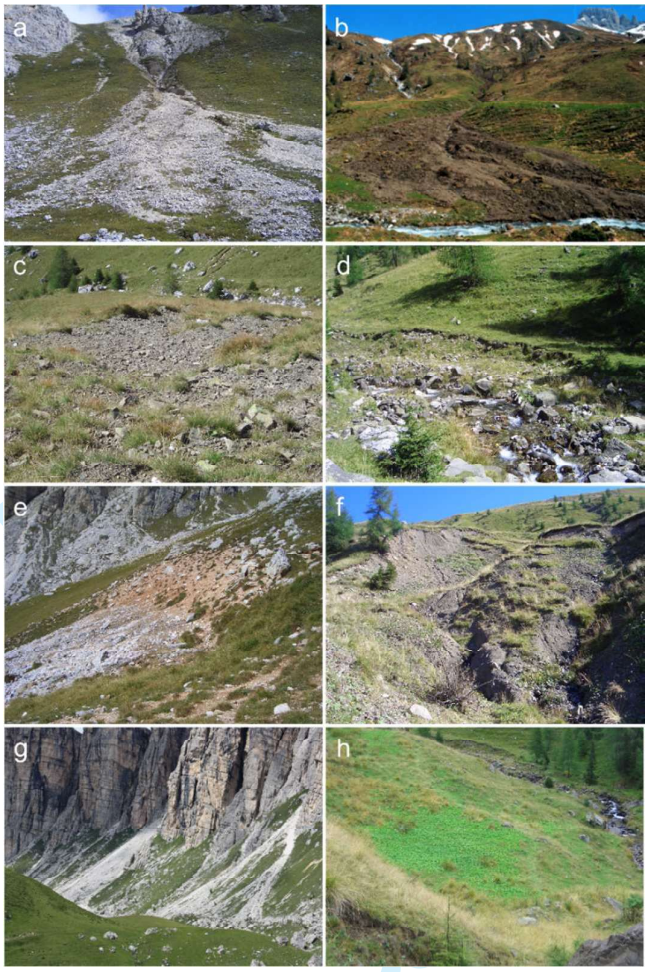

Figure 2: Different types of sediment source areas mapped in the Rio Cordon basin: debris flow-channel and –deposit (a); mud flow deposit generated by the evolution of a landslide occurred in 2001 (b); erosional area (c); eroded stream bank (d); shallow landslide (e); landslide which occurred in 2001 (f); active talus (g). Small wetland areas (h) were also mapped.

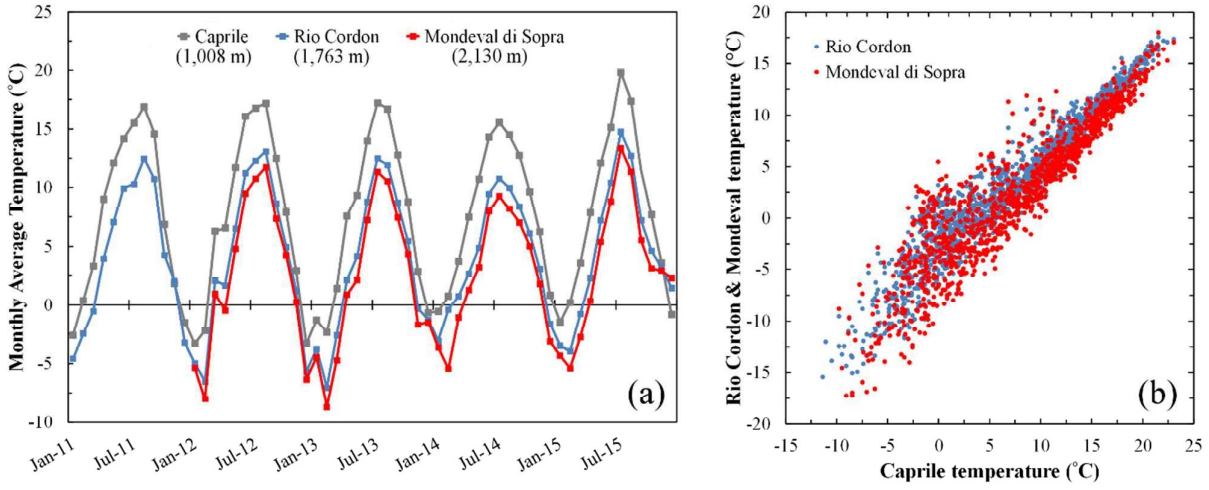

Figure 3: Monthly average air temperature in Mondeval di Sopra (2,130 m a.s.l.), Rio Cordon (1,763 m a.s.l.) and Caprile (1,008 m a.s.l.) (a). Rio Cordon – Caprile and Mondeval di Sopra temperature relationships (b).

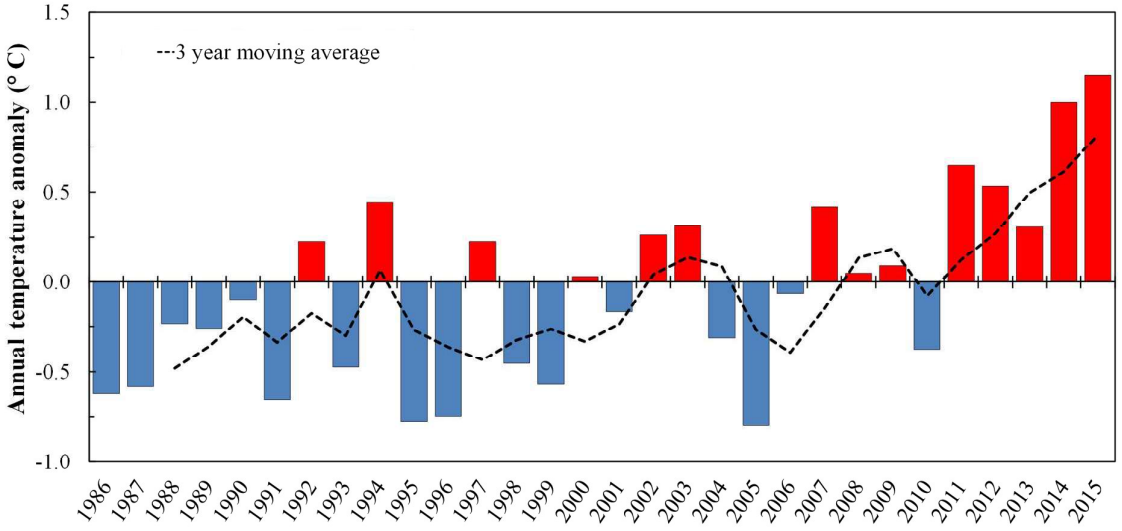

Figure 4: Average annual temperature in Caprile as the deviation from the 1986-2015 mean. Black dotted line is the 3 year moving average of the anomaly.

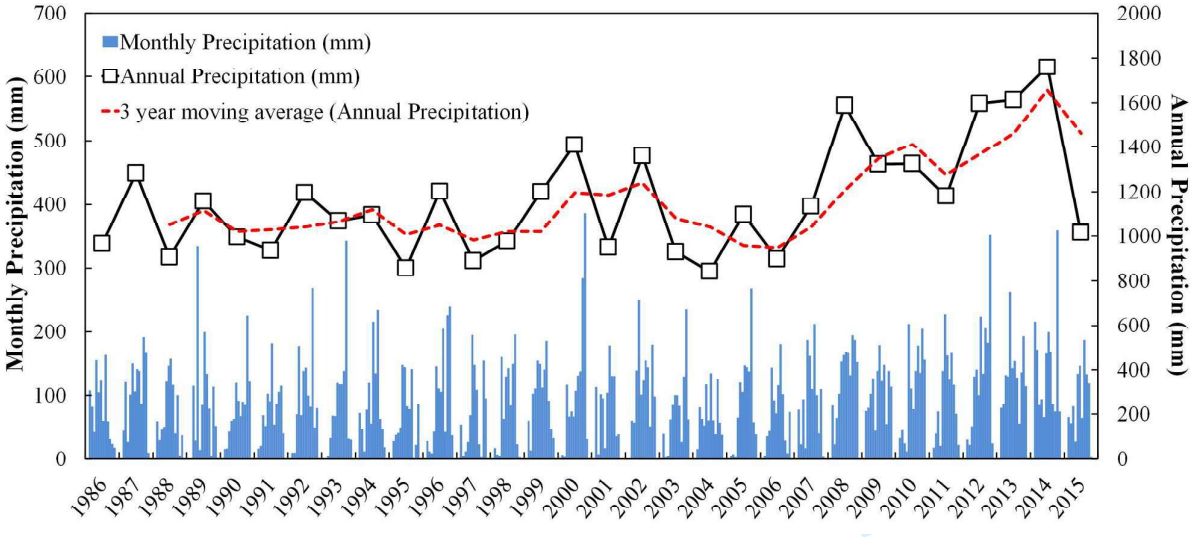

Figure 5: Monthly and annual precipitation in the Rio Cordon basin during the 1986-2015 period. The red dotted line is the 3 year moving average of the annual precipitation.

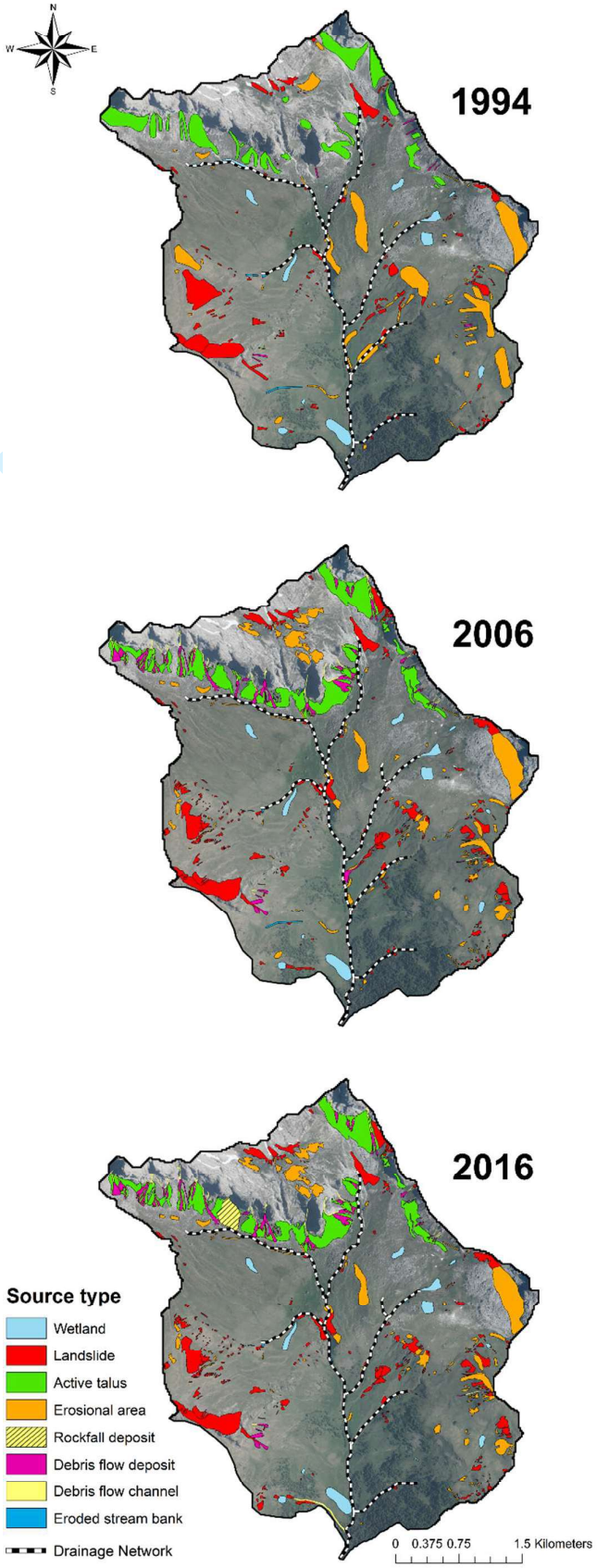

Figure 6: Sediment source inventories performed in the Rio Cordon basin in 1994, 2006 and 2016.

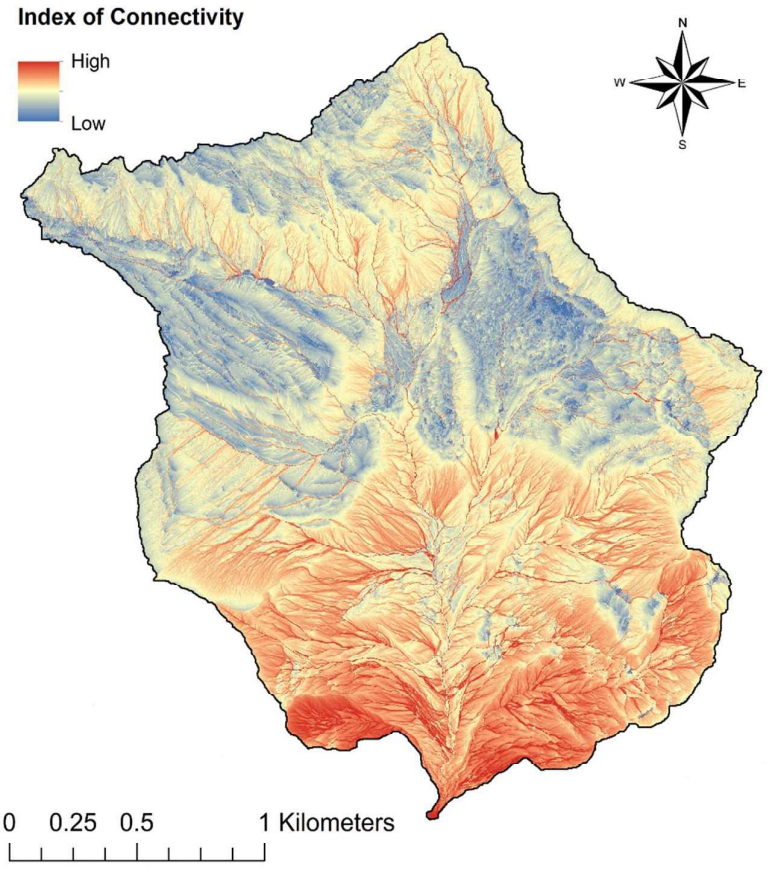

Figure 7: Sediment connectivity map

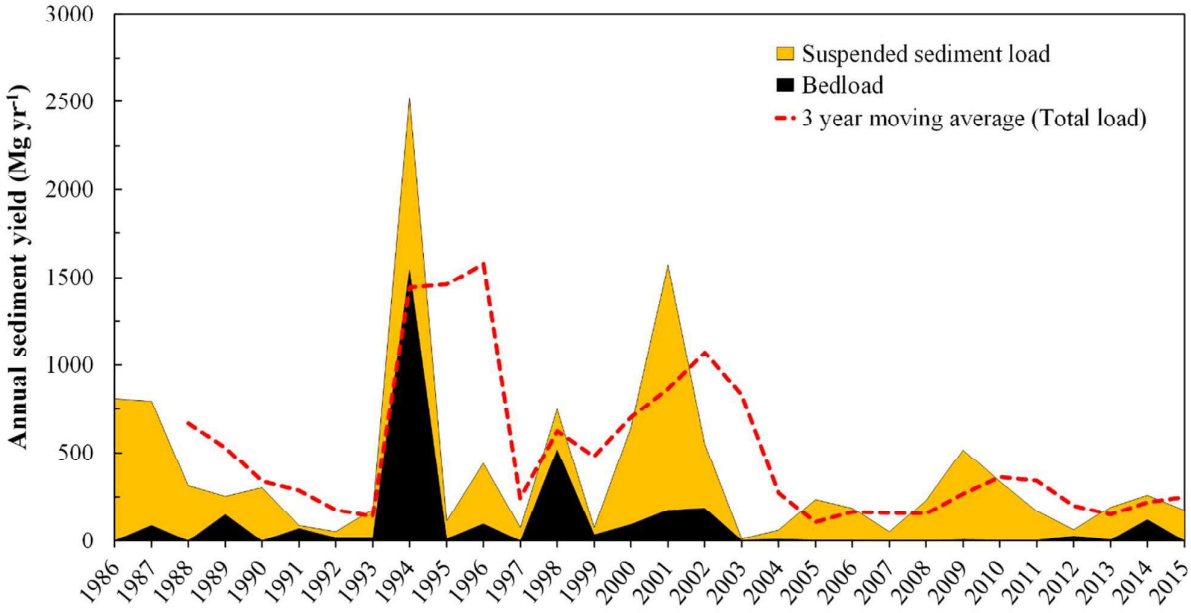

Figure 8: Annual sediment yield recorded by the Rio Cordon monitoring station during the 1986-2015 period. The red dotted line is the 3 year moving average of the total load (i.e. *SSL* + *BL*)

Table I: Mean annual air temperature and annual precipitation recorded in the 1986-2015 period at Caprile and Rio Cordon meteorological stations, respectively.

	Temperature (°C)	Rainfall (mm)
1986	6.3	967
1987	6.3	1281
1988	6.7	907
1989	6.6	1158
1990	6.8	996
1991	6.2	934
1992	7.1	1194
1993	6.4	1068
1994	7.3	1096
1995	6.1	856
1996	6.2	1200
1997	7.1	890
1998	6.4	976
1999	6.3	1200
2000	6.9	1409
2001	6.7	949
2002	7.2	1358
2003	7.2	930
2004	6.6	841
2005	6.1	1097
2006	6.8	898
2007	7.3	1134
2008	7.0	1587
2009	7.0	1322
2010	6.5	1325
2011	7.6	1180
2012	7.4	1597
2013	7.2	1612
2014	7.9	1757
2015	8.0	1016

Table II: Type, extent and evolution of sediment sources over the inventories performed in the Rio Cordon basin in 1994, 2006 and 2016. In 2006 and 2016, the debris flow type is the sum of the debris flow-channel and -deposit.

Type	1994			2006			2016		
	Area (m^2)	Count (n)	Av.area (m^2)	Area (m^2)	Count (n)	Av.area (m^2)	Area (m^2)	Count (n)	Av.area (m^2)
Debris flow	8887	10	889	71623	78	918	70816	78	908
- channel	*n/a*	*n/a*	*n/a*	*15340*	*38*	*404*	*18845*	*40*	*471*
- deposit	*n/a*	*n/a*	*n/a*	*56283*	*40*	*1407*	*51971*	*38*	*1368*
Erosional area	160241	66	2428	171050	98	1745	162406	85	1911
Eroded stream bank	5517	25	221	3902	22	177	1734	22	79
Landslide	149197	167	893	191797	195	984	195151	208	938
Active talus	174423	24	7268	210182	26	8084	201316	26	7743
Rockfall deposit	0	0	0	0	0	0	20676	1	20676
Total source areas	498265	292	1706	648554	419	1548	652100	420	1553
Wetland	46641	13	3588	43293	12	3608	43453	13	3343
Stabilized	*n/a*	*n/a*	*n/a*	2693	19	142	18773	33	569
Obliterated	*n/a*	*n/a*	*n/a*	*n/a*	*n/a*	*n/a*	10719	5	2144

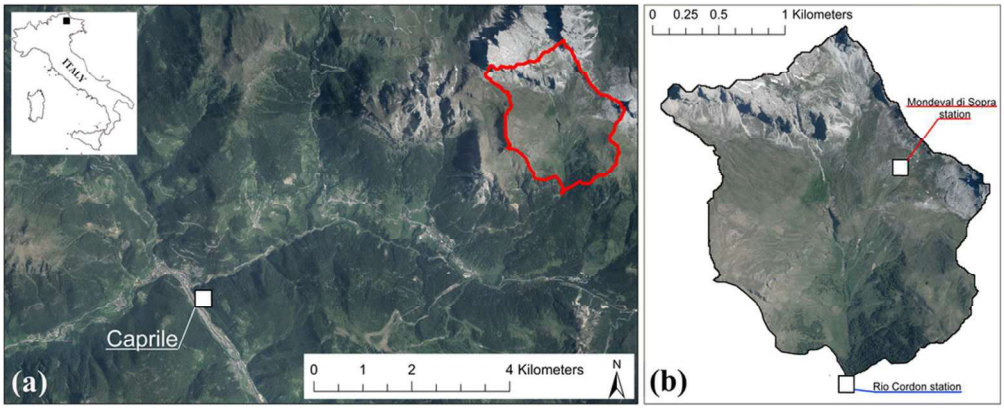

Figure 1: Location of the Rio Cordon basin (red outline) with respect to Caprile (a), and the Mondeval di Sopra and Rio Cordon stations in the basin (b). "Rio Cordon station" identifies both the meteorological and sediment transport monitoring station. The latitude-longitude (WGS84) of the Rio Cordon monitoring station are: 46.4505 N and 12.0953 E.

44x17mm (600 x 600 DPI)

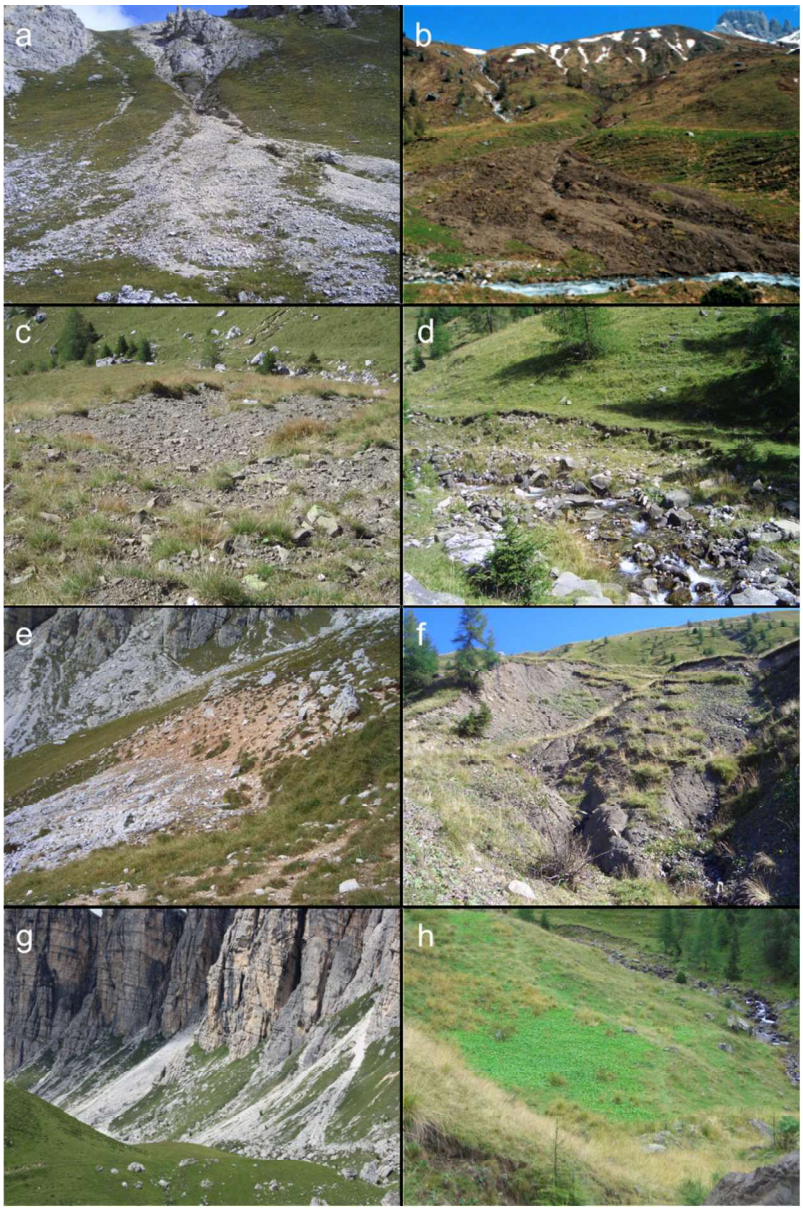

Figure 2: Different types of sediment source areas mapped in the Rio Cordon basin: debris flow-channel and –deposit (a); mud flow deposit generated by the evolution of a landslide occurred in 2001 (b); erosional area (c); eroded stream bank (d); shallow landslide (e); landslide which occurred in 2001 (f); active talus (g). Small wetland areas (h) were also mapped.

47x71mm (600 x 600 DPI)

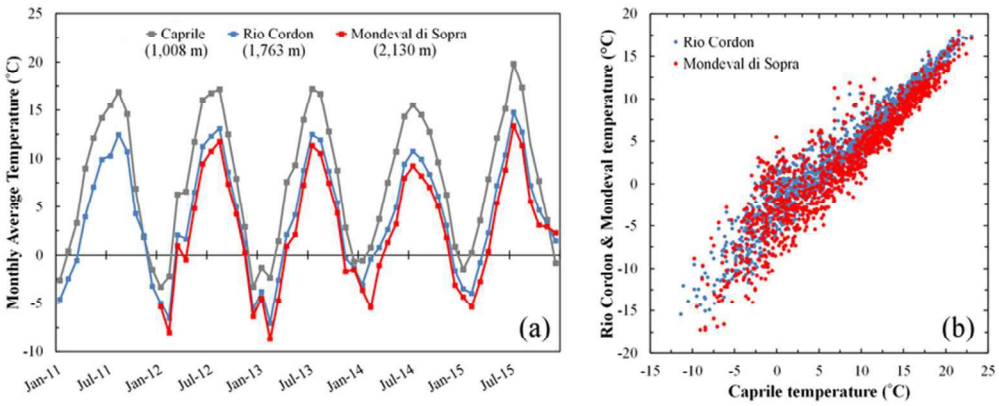

Figure 3: Monthly average air temperature in Mondeval di Sopra (2,130 m a.s.l.), Rio Cordon (1,763 m a.s.l.) and Caprile (1,008 m a.s.l.) (a). Rio Cordon – Caprile and Mondeval di Sopra temperature relationships (b).

36x14mm (600 x 600 DPI)

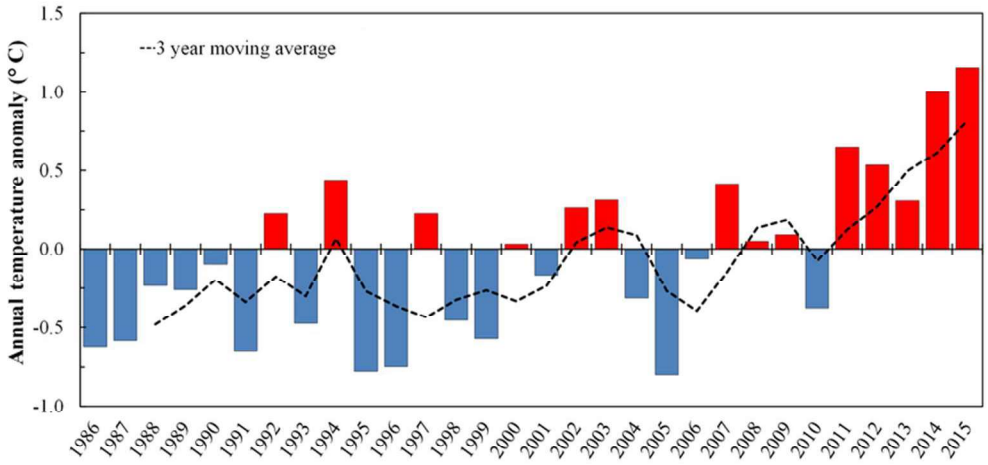

Figure 4: Average annual temperature in Caprile as the deviation from the 1986-2015 mean. Black dotted line is the 3 year moving average of the anomaly.

36x17mm (600 x 600 DPI)

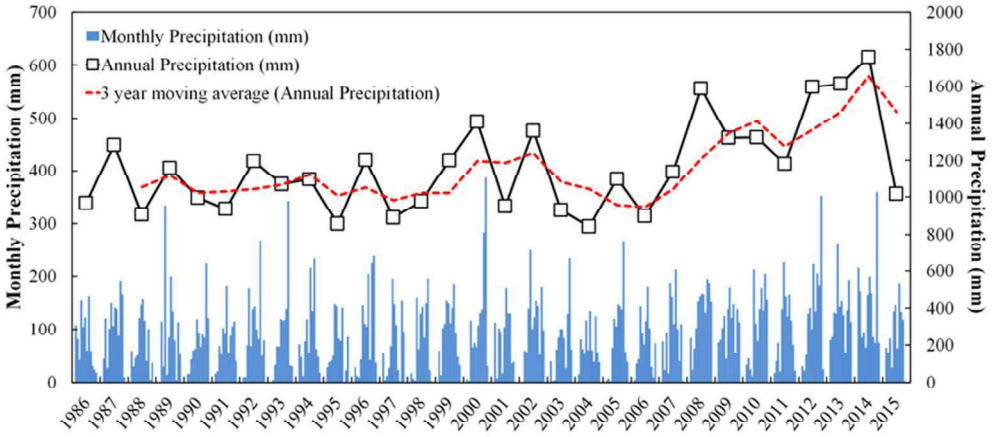

Figure 5: Monthly and annual precipitation in the Rio Cordon basin during the 1986-2015 period. The red dotted line is the 3 year moving average of the annual precipitation.

36x16mm (600 x 600 DPI)

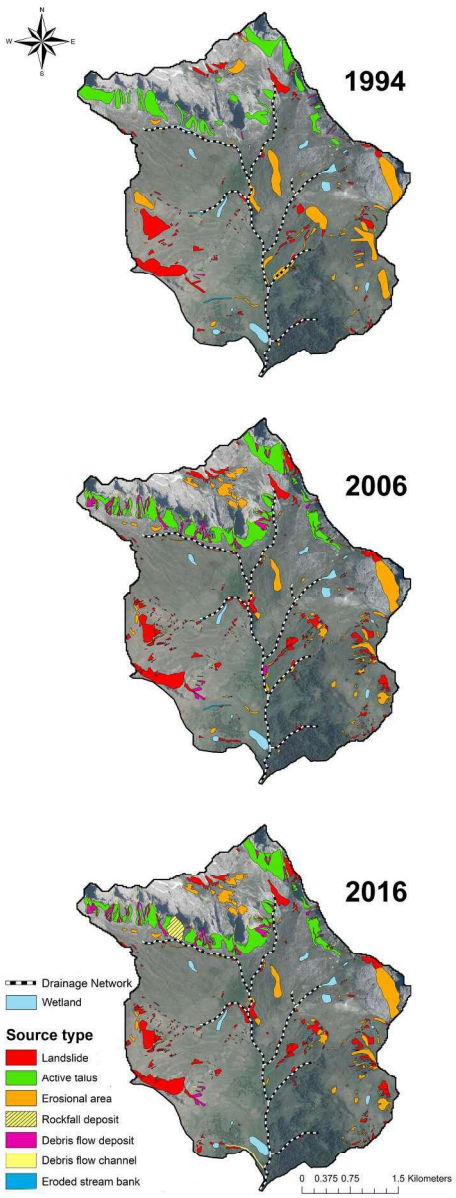

Figure 6: Sediment source inventories performed in the Rio Cordon basin in 1994, 2006 and 2016.

112x300mm (600 x 600 DPI)

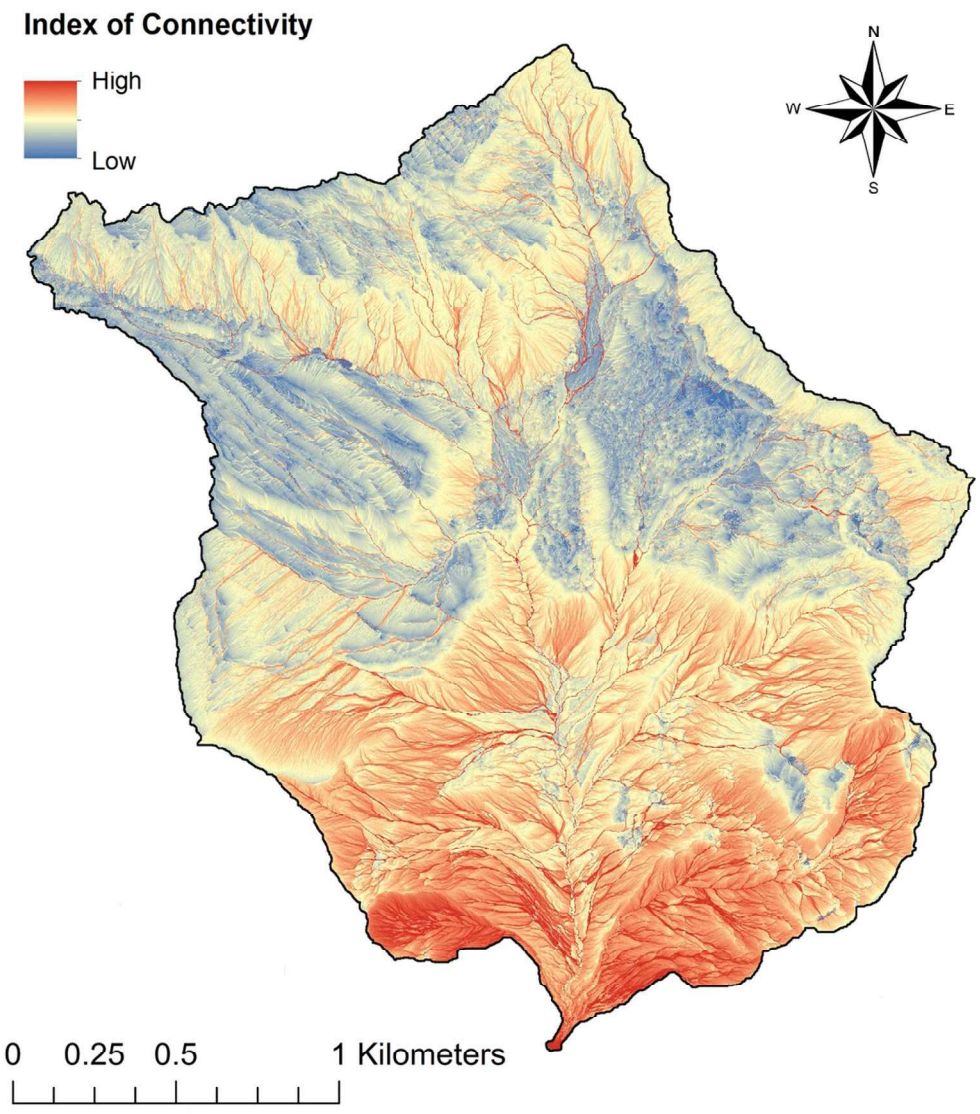

Figure 7: Sediment connectivity map

53x59mm (600 x 600 DPI)

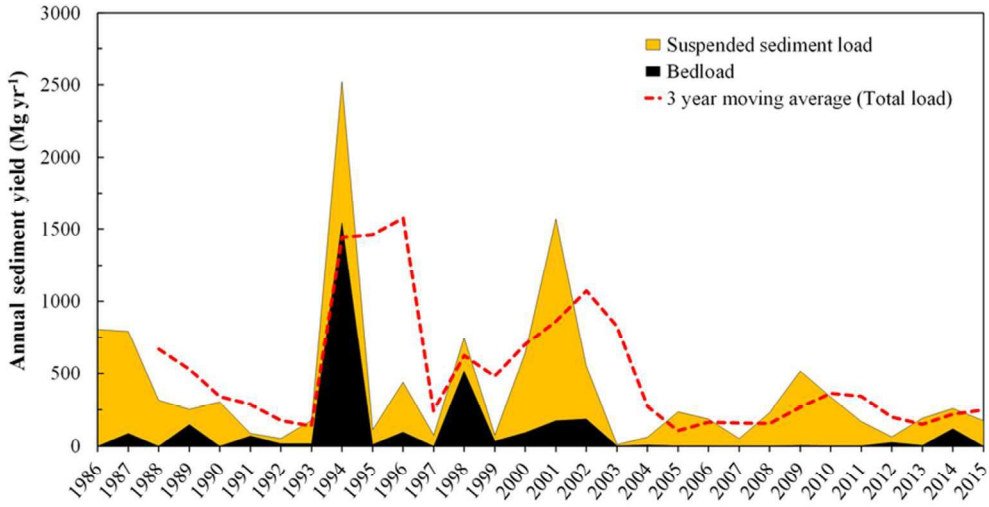

Figure 8: Annual sediment yield recorded by the Rio Cordon monitoring station during the 1986-2015 period. The red dotted line is the 3 year moving average of the total load (i.e. SSL + BL)

38x19mm (600 x 600 DPI)